Developing non-heat treated UHPC with local materials

Jin Zang, G P A G van Zijl

Department of Civil Engineering, Stellenbosch University, South Africa

This is an original scientific paper published in Concrete Beton, journal of the Concrete Society of Southern Africa, in Volume 142, pp 12-23, September 2015.

Journal Contact Details:
PO Box 75364
Lynnwood Ridge
Pretoria, 0040
South Africa
+27 12 348 5305

admin@concretesociety.co.za
www.concretesociety.co.za

Developing non-heat treated UHPC with local materials

Jin Zang and van Zijl G.P.A.G.*
Department of Civil Engineering, Stellenbosch University, South Africa

ABSTRACT

Non-heat treated ultra-high performance concrete is developed in this contribution, using locally available ingredient material except imported high-strength short steel fibre. While UHPC mix design guidelines have been proposed, ingredient materials available locally but which do not necessarily comply with recommended property ranges, may be compensated for by particular strategies. In this paper, the local ingredient materials are compared based on their mineralogy, specific surface area, particle size and grading. A mix design strategy is proposed and demonstrated, making use of local binder materials and fine aggregate with less than optimal properties. Base paste spread and strength are integral to the design, as is careful consideration of fibre size and dosage to ensure tight packing in the UHPC skeleton. Significant compressive strength enhancement by addition of the fibres is recorded, ascribed to the tight skeleton packing and shrinkage-induced fibre bond enhancement.

Keywords: UHPC, fibre reinforced, non-heat treated, local materials

1. INTRODUCTION

Ultra-high performance concrete (UHPC) without heat treatment has been developed successfully by several researchers. However, under such normal water curing conditions, the ingredient materials should meet tight specifications. When locally available materials are not that ideal, it is challenging to achieve the required performance. For the local materials in South Africa, the optimised mix design for UHPC from other researchers is no longer valid. In order to develop UHPC with the local materials, a good understanding of UHPC is needed and a systematic experimental design approach is required due to lack of corresponding data. This article presents a step by step development of UHPC with maximal use of local materials, i.e. all but the steel fibres. The major philosophy in the mix design is to identify strength potential of paste at early age, i.e. 14 days, and optimal design of fibre reinforcement for bridging of shrinkage-induced micro-cracks whereby fibres are mobilised already in the ascending response to mechanical load such as in the compression test and not only to reduce post-peak brittleness. Using this philosophy, the development of UHPC with 28-day compressive strength of 168 MPa, using local, non-ideal materials and normal water curing is elaborated in this paper.

**Corresponding author. Address: Department of Civil Engineering, Stellenbosch University, Private Bag X1, Stellenbosch 7602, South Africa*
Tel: +27 21 808 4369
E-mail addresses: jinzang2015@gmail.com (Jin Zang), gvanzijl@sun.ac.za

2. COMPARING LOCAL MATERIALS WITH TYPICAL MATERIALS USED FOR UHPC

In order to compare the differences in ingredient materials for UHPC, the relevant properties of local materials are introduced and compared with those used by other researchers who successfully develop UHPC under normal curing conditions.

2.1. Cement used in UHPC

Cement is the most important material in UHPC because the hydration of cement provides the fundamental way to achieve concrete strength. It is found that little C_3A content minimizes water demand (de Larrard 1988) which in turn will affect the viscosity of the paste. In addition, the fitness also governs the viscosity of paste (Bonen, Sarkar 1995). Sakai *et al*. (2008) state that the cement with less than 8 weight percentage of the C_3A content according to Bogue analysis does not have a significant influence on the paste viscosity. The above considerations of other researchers could be used as a reference to select cement that is better suitable for UHPC. As shown in Table 1, the cement used for this research is a CEM I 52.5N with 6.8% of C_3A content, which meets this requirement.

The hydration of cement determines the paste strength, which in-turn affects the UHPC strength. The researchers normally choose cement with high C_3S and C_2S contents. The typical C_3A, C_2S and C_3S contents in cement used for UHPC by researchers are listed in Table 1 for comparison.

Each researcher listed in Table 1 optimized their UHPC mix to enable workable fresh UHPC and the highest strength. It can be seen that UHPC strengths over 150 MPa choose cement containing similar percentages of C_3A and C_3S. The UHPC developed by Montreal has similar C_3S and C_2S contents compared with the local CEM I 52.5 N but contains much

Table 1: Cement major chemical contents and corresponding compressive strengths for UHPC.

28 days Strength (MPa)	Cement weight % according to Bogue analysis			Reference
	C_3A	C_3S	C_2S	
165 (water curing)	4.11	67.23	14.5	France (de Larrard, Sedran 1994)
168 (water curing)	4	73.4	10	Lausanne (Habel et al. 2006)
192 (without steel fibre) 201 (2.5 % by volume of steel fibre)	5	74.3	14.1	U.S. (Wille et al. 2011)
121 (water curing)	2	60	16	Montreal (Habel et al. 2008)
128 (water curing)	9	60	10	Toronto (Habel et al. 2008)
126 (water curing)	N/A	N/A	N/A	U.S. (Graybeal 2006)
168 (water curing)	6.8	61.6	17.2	CEM I 52.5 N in 2012; this research
128.6 (without steel fibre)	7.26	59	19	CEM I 42.5 N in 2011; this research

less C_3A content. The cement used in Toronto has similar C_3A and C_3S contents with this research but contains less C_2S content. The UHPC in both Montreal and Toronto achieves the compressive strength of less than 130 MPa, i.e. significantly lower than that achieved by the same lead author Habel *et al*. (2008) of 168 MPa in an earlier work, which emphasizes the importance of cement in UHPC.Habel *et al*. (2008) point out that most cements used in Europe contain approximately 4% of C_3A and 73% C_3S which enable good workability and strength development. The worst workability was found for cement containing 7% C_3A, which was discarded when UHPC was developed in Montreal. This finding differs from that of Sakai *et al*. (2008), who indicate that less than 8% C_3A does not have significant influence on paste workability. The one local cement used in this paper, CEM I 52.5N, contains 6.77% C_3A and was also found to cause a relatively low workability compared with that of Wille *et al*. (2011), which agrees with the finding by Habel *et al*. (2008). The detailed information will be provided in the later section.

Of the two types of cements used in this article, which are CEM I 42.5N and CEM I 52.5N, only the latter leads to sufficient compressive strength to be classified as UHPC. The major Bogue analysis of local cements are listed in Table 1.

2.2. Silica Fume

Silica fume normally has two functions in UHPC. One is its pozzolanic reaction that further enhances the concrete strength. The other is its physical role as a filler between cement particles.

From the physical point of view, the grain size of silica fume influences the packing of the paste. Wille *et al*. (2011) found that medium grain size of silica fume with specific surface area of 12.5 m^2/g has better effect on the workability and compressive strength than the common silica fume with specific surface area of 21.9 m^2/g. Habel *et al*. (2008) confirm that a relatively high specific surface area (15-20 m^2/g) of silica fume they use causes a high water demand and thus does not perform as well as the silica fume used in Europe with specific surface area of 12 m^2/g. Thus it appears that silica fume with specific surface area of approximately 12 m^2/g is the best option to be used in UHPC. However, only one type of grey silica fume with specific surface area of 23 ± 3 m^2/g and silica content over 92 percentage is available in South Africa. This is shown in a later section to have significant influence on UHPC workability.

2.3. Superplasticizer

Very low w/c ratio's make superplasticizer (SP) essential for UHPC to achieve the required good workability and spread. The SP used for UHPC is normally based on polycarboxylate ether containing different lengths of side chains (Schroefl *et al*. 2008). The side chain density is the main mechanism of controlling the workability of the paste (Zingg *et al*. 2009). Due to the chemical reaction between SP and cement/silica fume, different types of SPs are usually compatible with the corresponding cement and silica fume. The SP based on methacrylic acid ester polycarboxylate disperses cement better than silica fume while the allylether based polycarboxylate fluids silica fume well. Therefore, a blend of SPs that could both effectively disperse cement and silica fume are preferred in UHPC mix (Plank *et al*. 2009). In order to achieve a highly flowable paste, effective dispersion of especially silica fume is necessary (Plank *et al*. 2009).

The dosage of SP used for UHPC mix also contributes to the compressive strength. Different amounts of SP were compared and it was found that a lower percentage of SP leads to a reduced shrinkage rate which in turn results in a higher strength (Morin *et al*. 2001). Therefore, if the SP is not efficient in dispersing cement and silica fume, the addition of more SP might cause a higher shrinkage and result in a reduction in UHPC strength.

Although the theoretical role of the types of SP matching the types of cement and silica fume were studied well by researchers as discussed above, the side chain length and density is normally kept secret by chemical companies and no detailed information could be obtained in this research. For this reason, there are no simple chemical balance equations from which to derive the optimal dosage, but a systematic, empirical test program was followed to measure spread values representing the workability of paste, following (Artelt, Garcia 2008).

Four locally available types of SPs were used in this research are marked SP I to SP IV, and were obtained from three local supplier companies. The best performance of SP is determined through slump flow / spread value results for the test mixes reported here.

2.4. Fine Aggregate

2.4.1. Aggregate particle size

Aggregate in concrete mix usually is not involved in chemical reactions. For UHPC, the larger grain size aggregate can influence compressive and tensile strength due to stress concentrations caused by a relatively high shrinkage of paste compared with normal strength concrete. Therefore, most researchers choose fine sand as aggregate in UHPC under normal curing conditions. This is in agreement with de Larrard & Tondat (1993) who indicate that a small size aggregate leads to a higher strength in high strength concrete. The sands used by some researchers who successfully develop UHPC under normal curing conditions are listed in Table 2 below.

Table 2: Types of sand used by some researchers for water cured UHPC

Reference	Sand types and particle sizes
France (de Larrard, Sedran 1994)	Three type of quartz sand S125, S250 and S400 are used. S125 range between 0.063 mm and 0.125 mm; S250 range between 0.1 mm and 0.25 mm; S400 range between 0.125 mm and 0.4 mm;
Switzerland (Habel et al. 2006)	Quartz sand with the maximum grain size of 0.5 mm.
U.S. (Wille et al. 2011)	Two types of fine silica sand with the maximum grain size of 0.2 mm and 0.8 mm respectively.
Montreal (Habel et al. 2008)	Silica sand with the mean grain size of 0.25 mm.
Toronto (Habel et al. 2008)	Silica sand with the mean grain size of 0.2 mm.
U.S. (Graybeal 2006)	Fine sand with grain size range between 0.15 mm and 0.6 mm.

It can be seen from Table 2 that most of the researchers choose fine sand of grain size approximately between 0.2 and 0.8 mm. The sand from most researchers was supposed to be obtained from their local suppliers but whether the sand is re-graded or not is not reported in their research. This research will only use the local available sand as aggregate instead of sieving and re-grading them.

Two types of natural sands, Philippi and Malmesbury that are commonly used in the Western Cape, South Africa are chosen. The gradings of these sands are shown in Figure 1. Malmesbury sand is generally preferred for normal concrete due to its wider range in particle sizes. However, it contains particles larger than 2.4 mm while all Philippi sand particles pass through the 1.2 mm sieve.

Figure 1: The grading of two types of sands used in this research.

2.4.2. Aggregate grading

Better graded aggregate also helps to reduce the dimensional change due to shrinkage. The aggregate has a positive confinement effect on the cement paste (de Larrard, Sedran 1994) which indicates that the aggregates act as an internal restraint to reduce the shrinkage. Other researchers indicated that better graded aggregate could reduce the volume of cement paste which results in a lower chemical shrinkage (Holt 2001, Esping 2007). Such confinement of aggregate is especially helpful for UHPC because of the relatively high paste shrinkage.

2.4.3. Aggregate particle shape

Besides the grading, the shape of the aggregate also contributes to the workability of concrete. For the similar grain size, well-rounded smooth sands flow much better than the angular sand during the mixing procedure and lead to fewer voids in the UHPC performance. Therefore, well-rounded, smooth sand particles are better suited for UHPC. Enlarged photos of sand particles from the various size ranges are shown in Table 3.

The particle shape for each size is shown in Table 3 with magnification up to a factor of about 200 for better observation. For the very fine size (< 75 µm), the shape of Malmesbury sand appears to be more rounded than that of Philippi sand. However, for the sand size larger than 75µm, the shape of Philippi sand particles is better than that of Malmesbury sand.

2.5. Steel Fibre

Short high strength steel fibres are normally used in UHPC. Since no South African company manufactures high strength steel fibres yet, the steel fibres are imported. Bekaert straight steel fibre of 13 mm in length, 0.16 mm in diameter with a minimum tensile strength of 2600 MPa and brass coating is used in this research. Steel fibres used for UHPC by different researchers are similar and are commonly used to improve the ductility of UHPC.

Table 3: Particle shapes for two South African sand types.

Size (Micron)		Phillipi		Malmesbury	
Between		Photo	Magnification	Photo	Magnification
2360	4750				34
1180	2360		35		55
600	1180		35		42
300	600		173		176
150	300		181		184
75	150		195		195
<75			203		199

2.5.1. The effect of short straight steel fibre content on UHPC performance

Usually, steel fibres mainly improve concrete ductility. This is because only once the concrete cracks, the fibre is significantly stretched to develop resistance in bridging the crack. Therefore, the steel fibre has limited effect on concrete cracking strength, whether in (splitting) tension or compressive splitting.

The effects of steel fibre content on UHPC are different under various curing conditions. Park *et al*. (2008) found that 2% (by volume) of steel fibre results in a 13% improvement in compressive strength under heat curing conditions. For non-heat treated UHPC, an improved compressive strength of 6.7% is achieved with 1.5% (by volume) of steel fibres and an improved compressive strength of 9.8% is obtained with 2.5% steel fibres (Wille *et al*. 2012). It can be seen from work of other researchers that the effect of steel fibres on UHPC compressive strength is less significant under the normal curing conditions as that of the heat curing conditions. In addition, lower steel fibre content results in a lower improvement in compressive strength for UHPC.

2.5.2. The spacing and dispersion of steel fibres in UHPC

The effects of fibre dimension and content on fibre spacing were studied by several researchers, who also proposed formulae for fibre spacing. Among those formulae, the typical expression for continuous fibre is shown as Equation (1) (Romualdi, Mandel 1964); the expression that considers the length of short steel fibres is shown in Equation (2) (Mindess, Young 1981) and the spacing for random oriented steel fibres in Equation (3) (McKee 1969). Equation (3) was

also accepted in European standard EN 14487-1 as a requirement for minimum dosage of steel fibres used in fibre reinforced concrete (FRC) to ensure minimum overlap between fibres.

Despite the fact that the fibre spacing expressions were originally used to evaluate the tensile behaviour of FRC, they might also be used as an indication to choose the maximum aggregate size (Markovic 2006). However, the actual dispersion of fibres is more complicated and it is unlikely that fibres arrange in a complete regular grid as assumed by the formulae. The factors that affect fibre dispersion include: the confinement of formwork, fibre size and content, aggregate size, matrix viscosity, vibration, etc. Researchers are developing models that could better simulate the fibre dispersion but there are still quite some limitations. However, it is useful to consider theoretical steel fibre dispersion in the mix design.

$$S = 13.8d\sqrt{\frac{1}{V_f}} \qquad (1)$$

$$S = 13.8d\sqrt{\frac{l_f}{V_f}} \qquad (2)$$

$$S = \sqrt[3]{\frac{nd^2 l_f}{4V_f}} \qquad (3)$$

with:

S fibre spacing, d fibre diameter, l_f fibre length and V_f volume content of steel fibres in %.

Figure 2 shows the relationship between the volume percentage of steel fibres and fibre spacing as obtained from the above three expressions. The maximum aggregate size that better fits between steel fibres differs significantly when the steel fibres content is low and such variation narrows when the steel fibre content is high.

It can also be seen from Figure 2 that for Equation (3), the fibre spacing does not change that much with different percentage of steel fibres since the main focus for this expression is to guarantee enough overlap of steel fibres. The fibre spacing for Equation (2) becomes more constant after 3% of steel fibres, while for Equation (1), the fibre spacing reduces with the increased volume percentage of steel fibres and has a high decreasing rate when the steel fibre content is less than 3%.

In order to provide a good dispersion of steel fibres, the fibre length should be typically 2 to 4 times that of the maximum aggregate size (Grünewald 2004). For Malmesbury sand, approximately 98% of the particles are smaller than 2.36 mm according to the sieve test (Figure 1), which complies with the above fibre length requirement. In addition, based on Equation (2), a 1.5% by volume of steel fibre corresponds to approximately 2 mm of maximum sand particle size. Besides the relationship between fibre spacing and maximum aggregate size, the fibre spacing should be lower than 0.45 l_f for a minimum overlap according to EN 14487-1 and Equation (3). With 1.5% of steel fibres, the fibre spacing is approximately 0.56 mm as shown in Figure 2, which is smaller than 0.45 l_f (= 5.85 mm) and meets the requirement.

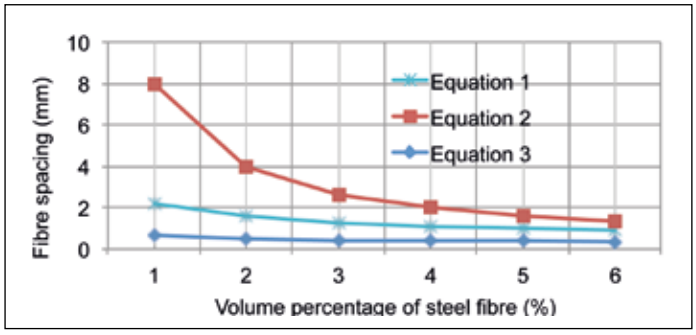

Figure 2: Fibre spacing corresponding to volume percentage of steel fibre.

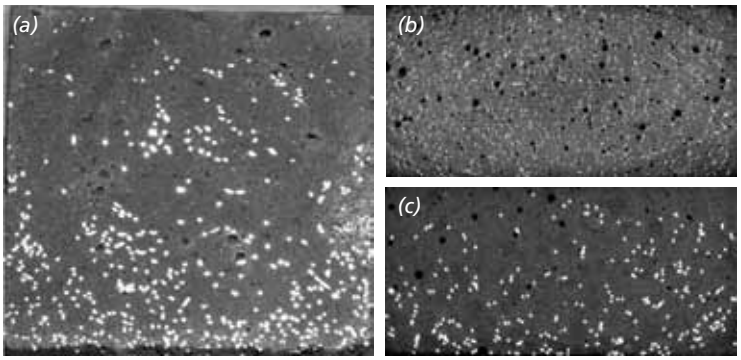

Figure 3: Steel fibre dispersion in (a) fine aggregate concrete (Głodkowska, Kobaka 2013); (b) 40mm thick dumbbell shaped specimen with moderate vibration (this research); (c) 16mm thick dumbbell shaped specimen with excessive vibration (this research).

Based on the above analysis, a 1.5 volume percentage of steel fibre was chosen in this research. In this way, a uniform dispersion of steel fibre is expected. By balancing the particle size and fibre spacing, this research aims to exploit good fibre packing as part of a tight skeleton, whereby paste shrinkage-induced anchorage may lead to significant fibre-enhanced compressive strength.

2.5.3. Steel fibre dispersion in UHPC

As can be seen in Figure 3 (a), the actual dispersion of steel fibres in fine aggregate FRC with 1.5 volume percentage of steel fibres in 150 mm cube specimens may be non-uniform, and thus not ideal as in equations (1-3). The settling of steel fibres is caused by the combined effects of steel fibre gravity, viscosity and vibration time (Głodkowska, Kobaka 2013). The phenomenon of steel fibre settlement was also observed with longer vibration times in this research. Figure 3 (b) shows the steel fibre dispersion in a 40 mm thick dumbbell shaped specimen with the vibration time of one minute, while Figure 3 (c) shows a 16 mm thick dumbbell shaped specimen with the vibration time of two minutes. It can be seen from Figure 3 (c) that with longer vibration time, the steel fibre settlement tends to occur. Moderate vibration may prevent steel fibre settlement as shown in Figure 3 (b), which indicates good dispersion of steel fibres in this research under such considerations.

Besides the fibre dispersion, voids in UHPC can be eliminated with longer vibration time. This can also be observed when comparing Figure 3 (b) and (c). The location of voids close to the top surface of the specimen in Figure 3 (c) indicates that longer vibration time does help to reduce the voids. Settlement of steel fibre should however be avoided in structural application.

3. THE PHILOSOPHY OF UHPC DESIGN IN THIS RESEARCH

Guidelines for developing UHPC have been proposed by several researchers and are not repeated here. However, adaptations to accommodate local ingredient materials are elaborated. The major difference for UHPC developed in this research is to use steel fibre not only to improve ductility, but to also significantly contribute to compressive strength by confinement and internal pre-stressing.

The optimised paste may exhibit suitably high compressive strength at relatively early age, i.e. at 7 or 14 days, but reduced apparent strength at higher age, when testing compressive strength of the paste (UHPP) only. This strength reduction is postulated to be mainly caused by a relatively high shrinkage potential of the paste, internal water consumption by hydration and associated shrinkage strain gradients and internal cracking in the compression test specimen. The added aggregate is usually optimised for a tight packing to form a dense skeleton of the UHPM. This may further restrain shrinkage of the paste and cause apparent strength reduction due to internal cracking. The inclusion of an appropriate size and dosage of fibre contributes to the dense skeleton in the final composite (UHPC). Upon shrinkage of the paste, its tensile strain and associated stress is balanced by compression in the skeleton. By this confining skeleton pressure, anchorage of the fibres is improved. When tensile strength of the restrained shrinking paste is exceeded, tightly embedded fibres may efficiently bridge subsequent micro-cracks. For this mechanism to successfully enhance composite compressive strength, tightly packed, uniformly dispersed fibres with sufficient overlap are required to avoid weak spots that may lead to localized micro-crack coalescence and associated apparent low compressive resistance.

For UHPC, chemical shrinkage dominates at early age, i.e. within 24 hours. After a short period of time, the skeleton of the UHPC is strong enough to resist the shrinkage force, whereby the subsequent autogenous shrinkage strain is reduced (Holt 2001). Normal cured UHPC, such as studied here, shows a continuous shrinkage evolution, while heat-cured UHPC exhibits no evident post-treatment shrinkage (Graybeal 2006). Shrinkage observations in water-cured UHPC reported by Schachinger, *et al*. (2002) indicate autogenous strain in UHPC of approximately 0.14% within the first 24 hours, after which it develops slowly to approximately 0.16% at 7 days. After 7 days, the gradient of autogenous strain is larger, where the micro-cracks may be developed. Especially with low silica fume to cement content ratio of 0.18, a slight drop of autogenous strain occurs in 14 days. This may explain the reduction in UHPP strength at higher age found in this research.

For the paste of w/c ratio of 0.3 and SF/C = 0.10, shrinkage-induced clamping pressure on steel fibre increased significantly with the shrinkage development; the increments in clamping pressure are especially high until 210 hours after casting and continued increase its value until 500 hours when the test is stopped (Stang, 1996). Such improved bond stress induced by improved shrinkage further indicates the higher UHPP strength at 7 or 14 days is quite important to form a strong skeleton.

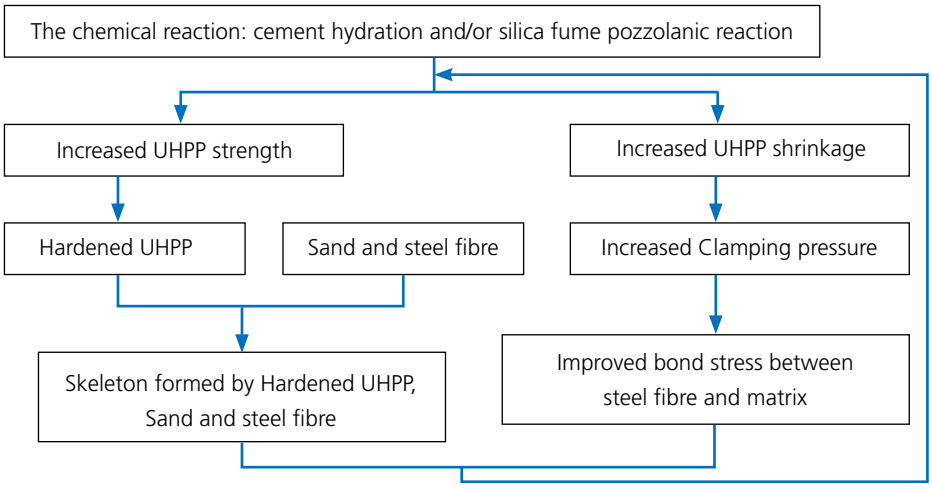

Figure 4: Skeleton formation procedure.

By following the iteration process in Figure 4, the skeleton starts to forms and grows stronger with the increase of UHPP strength. With a quick UHPP strength development up to 14 days, the skeleton becomes stronger and the pre-stressing force in steel fibre becomes larger. After 14 days, the strength of UHPP starts to degrade mainly caused by a relatively higher shrinkage as elaborate above. The formed strong skeleton up to 14 days, enough clamping pressure and lap length, all make steel fibre able to balance differential stress, or micro-cracks may develop in later days.

An advantage of the mix design followed here is that it uses paste shrinkage to its advantage for fibre activation. Other researchers improve strength by adding internal water reserve for continued hydration and

Table 4: UHPC phased design, showing Phase I-UHPP, Phase II-UHPM, Phase III-UHPC

Step	UHPC mix ingredients									Slump (mm)		f_{cu} (MPa)				
	Fibre	S/C		Aggr	SP			SF/C	w/c	CEM I		CEM I				
	V_f (%)	P	M	6mm	%	% s	Type			42.5N	52.5N	42.5N	52.5N	Age	No.	Std
1a. w/c for UHPP strength					2.80	0.84	SP I	0.18	0.30	342.0		109.2		28	3	5.2
					2.80	0.84	SP I	0.20	0.30	326.0		113.0		21	2	1.0
					2.40	0.72	SP I	0.18	0.28	312.0		113.1		28	4	7.6
					2.80	0.84	SP I	0.18	0.28	327.0		118.2		21	2	1.7
					2.80	0.84	SP I	0.25	0.27	229.0		124.0		28	4	4.7
					2.80	0.84	SP I	0.18	0.26	321.0		125.2		28	4	4.4
					3.30	0.99	SP I	0.18	0.24	307.0		138.6		14	4	6.9
					5.50	1.65	SP I	0.18	0.22	320.0		143.9		14	4	2.3
					5.40	1.62	SP I	0.18	0.20	290.0		148.4		14	4	5.9
1c. SP type for UHPP spread					3.20	0.98	SP II	0.18	0.22	278.8						
					5.48	1.67	SP II	0.18	0.22	259.0						
					5.50	1.68	SP II	0.18	0.20	213.3						
					3.42	1.03	SP III	0.18	0.22	315.0						
					5.52	1.66	SP III	0.18	0.22	321.0						
					3.20	1.18	SP IV	0.18	0.22	345.3						
					5.50	2.04	SP IV	0.18	0.22	322.0						
					3.37	1.01	SP I	0.18	0.22	276.0						
					5.50	1.65	SP I	0.18	0.22	260.3						
1d. SF/C					3.20	1.18	SP IV	0.20	0.22		337.8					
					3.20	1.18	SP IV	0.18	0.22		346.3					
					3.20	1.18	SP IV	0.16	0.22		362.5					
					3.20	1.18	SP IV	0.18	0.20		309.3					
					3.20	1.18	SP IV	0.16	0.20		329.0					
1e. SP dosage					1.60	0.59	SP IV	0.16	0.20		278.5					
					2.40	0.89	SP IV	0.16	0.20		327.3					
					2.80	1.04	SP IV	0.16	0.20		336.5					
					3.60	1.33	SP IV	0.16	0.20		329.5					
					4.00	1.48	SP IV	0.16	0.20		323.3					
1b. Sand			0.8		6.80	2.04	SP I	0.18	0.22	225.0		119.5		28	3	3.5
			1.2		6.80	2.04	SP I	0.18	0.22	190.3		117.2		28	3	2.2
		0.2	0.6		6.80	2.04	SP I	0.18	0.22	228.3		122.5		21	1	
		0.8			6.80	2.04	SP I	0.18	0.22	216.0		128.3		21	1	
2: UHPM					2.81	1.04	SP IV	0.16	0.20		336.0		152.8	14	1	
			0.6		2.80	1.04	SP IV	0.16	0.20		294.3		144.3	21	1	
			1.0		2.80	1.04	SP IV	0.16	0.20		247.3		135.3	28	3	4.7
			1.4		2.81	1.04	SP IV	0.16	0.20		203.0		99.3	28	3	6.5
					2.80	0.85	SP II	0.16	0.20		266.5		135.3	28	3	3.1
			1.0		2.80	0.85	SP II	0.16	0.20		163.8		112.5	21	1	
			0.6	12%	2.82	1.04	SP IV	0.16	0.20				131.2	21	1	
3.UHPC	1.5		0.6		2.81	1.04	SP IV	0.16	0.20				168.7	28	3	3.5
	1.5		0.6	12%	2.82	1.04	SP IV	0.16	0.20				161.4	21	3	1.5

reduction in shrinkage of UHPC by addition of superabsorbent polymer (SAP) (Dudziak, Mechtcherine 2008), or a shrinkage reducing admixture (SAR) (Soliman, Nehdi 2014). In this paper, the shrinkage-induced fibre confinement and pre-stressing is exploited to achieve UHPC with modest fibre content, without such SAP or SAR additives.

4. SPECIMEN PREPARATION AND TESTING

The mixing procedure is similar to other researchers. Compressive strength tests were performed on 100×100×100 mm specimens in the first batch only and mixed with a 50L mixer with lid. The remaining batches of specimens were 50×50×50 mm cubes and mixed with a three-speed Hobart 10L bowl mixer. When the mix of UHPC is finished, the fresh UHPC is cast into a mould and vibrated for one minute. The specimens were covered with a plastic sheet and stored in the laboratory at room temperature for 48 hours. Then the specimens were de-moulded and stored in a water tank with the temperature of 23 ± 2°C until the test at an age of 28 days. A total of 8 specimens are cast in the first batch, of which two specimens are tested on the first two weeks and the remaining four specimens are tested on 28 days. The rest of the batches cast a total of 6 specimens, of which 1 specimen is tested for the first three weeks and the rest tested on 28 days. A Contest compressive materials testing machine with the capacity of 2000 kN was used to test the compressive strength.

Besides the compressive test, the workability of UHPP through spread value is also measured. The equipment used to measure the spread value of UHPP is a cone according to ASTM C230/C230M without compacting.

The measurement of UHPP is different from that of UHPM. As for the UHPP, the cone was located on a flat steel plate and filled with fresh UHPP. The top surface of the cone was levelled after filling the UHPP and no leakage was allowed between the cone and the plate. Upon removing the cone, the UHPP flowed under the gravity. Measurement of the flow diameter was taken after 1 minute. In order to minimize the error, four measurements were taken. The UHPM flow test followed ASTM C1437 procedures for layered filling of the cone and tamping, levelling the upper surface, removing the cone, dropping the table 25 times within 15 seconds and subsequently measuring the spread value.

5. STEP BY STEP DEVELOPING UHPC IN THIS RESEARCH

The design method entails three phases, namely

Phase 1: Design of high strength, yet sufficiently flowable UHPP;

Phase 2: Addition of fine aggregate which to form sufficiently strong, flowable UHPM;

Phase 3: Addition of suitable fibre and fibre volume to complement the skeleton in UHPC.

An iterative process may be required. This may be to redefine the flowability and/or strength threshold for the preliminary optimized UHPP composition if incompatibility between the paste and fine aggregate leads to UHPM of insufficient flowability or compressive strength.

In addition to compressive strength, the spread value of UHPP was evaluated through flow table tests, due to its efficiency in indicating optimised paste packing density (Wille *et al*. 2011). A threshold value of 300 mm was used while varying other paste ingredients of cement (C), silica fume (SF) and superplasticiser (SP) type and dosage for optimised strength.

The phases of design, together with detailed mix proportions, spread and compressive strength results, are summarized in Table 4. In the following sections, the steps towards deriving an UHPC mix using local materials but no heat curing, are elaborated.

5.1. Phase 1 - Optimization of the UHPP

Since the UHPP provides the chemical reaction that governs the compressive strength of UHPC, the mix design starts with the UHPP mix design, based on the established design guidelines of ingredient materials with desired physical and chemical characteristics and proportions elaborated in section 2 of this paper. Two types of local cement (denoted by C), a CEM I 42.5N and a CEM I 52.5N were considered. Local availability dominated this decision, with the preferred CEM I 52.5N becoming available only after Phase I in this research. The only type of local Silica fume (SF) was used.

5.1.1. Phase 1a: Role of w/c ratio

The role of w/c in UHPP compressive strength is shown in Figure 5a, for phase 1a. Increased strength is observed for reduced w/c values, while keeping the SF/C ratio constant at 0.18. Also shown is the increased

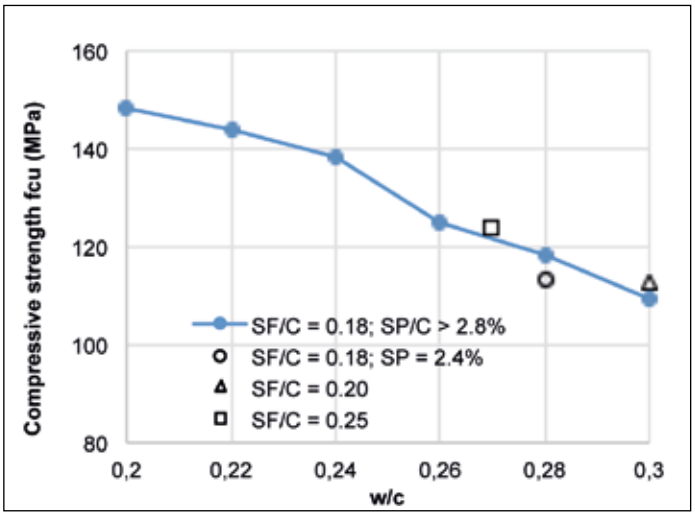

(a) Stage 1a max. strength vs w/c results

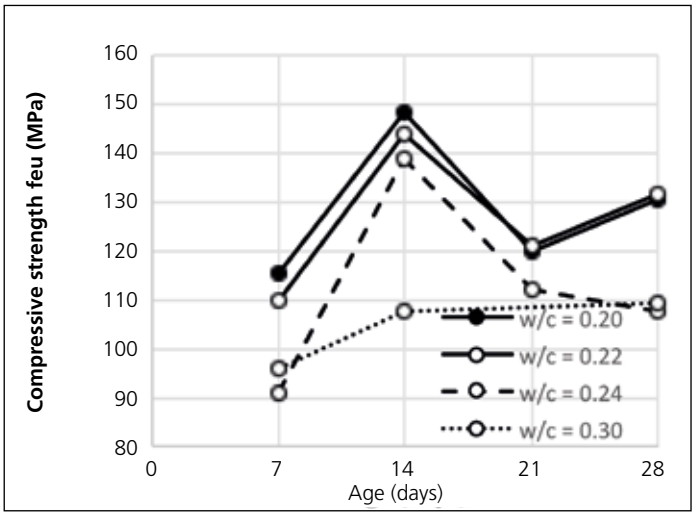

(b) Stage 1a: compressive strength development

Figure 5: UHPP compressive strength vs (a) w/c ratio and (b) test age up to 28 days.

strength for higher SF/C ratios of 0.20 and 0.25 at w/c ratios of 0.30 and 0.27 respectively. However, of importance is sufficient UHPP spread, as indication of good lubrication once fine aggregate and fibres are added. While slump flow of more than 300 mm could be obtained with reasonable amounts of SP for SF/C = 0.18, the flow values dropped significantly for increased SF/C values, with the extreme drop to 229 mm for SF/C = 0.25.

For the fixed SF/C = 0.18, when w/c ratio is under 0.24, the slump flow is much lower than 300 mm by direct addition of the full SP dosage. Step addition of SP, i.e. applying for instance half dosage at a time with continued mixing of several minutes in-between, can improve the slump flow compared with direct addition of SP (Tue *et al*. 2008). In order to achieve better slump flow, step addition of SP was used, but still the slump flow only reached 290 mm when w/c ratio is 0.2, indicating more efficient SP is needed. For the UHPP mixes with SF/C = 0.18 and w/c ratios of 0.24 and below, step addition of SP was followed in this work.

The strength evolution with curing time is shown in Figure 5b. When w/c = 0.30, the UHPP strength increases with time until 28 days. When the w/c ratio is below 0.24, it shows a drop in UHPP strength after 14 days. The slump flow is over 300 mm indicating that enough packing density is achieved with this UHPP. The reason for the drop in UHPP strength after 12 days is believed to be the high autogenous shrinkage, which by skeleton restraint causes internal tension and cracking.

The w/c ratio of below 0.24 is chosen for two reasons: The cement and SF are not as ideal as those researchers who successfully develop UHPC with w/c ratio of about 0.2. Secondly, the UHPP strength is too low for w/c = 0.3, with only 109 MPa in 28 days.

Therefore, the UHPP maximum compressive strength approaches 150 MPa for the base mix of w/c = 0.20, SF/C = 0.18 and sufficient amount of SP to achieve at least 300 mm slump flow. Improved slump flow may enable increased SF/C ratio, which was shown to hold potential for strength increase. Also, CEM I 52.5N should be used instead of the CEM I 42.5N to improve strength.

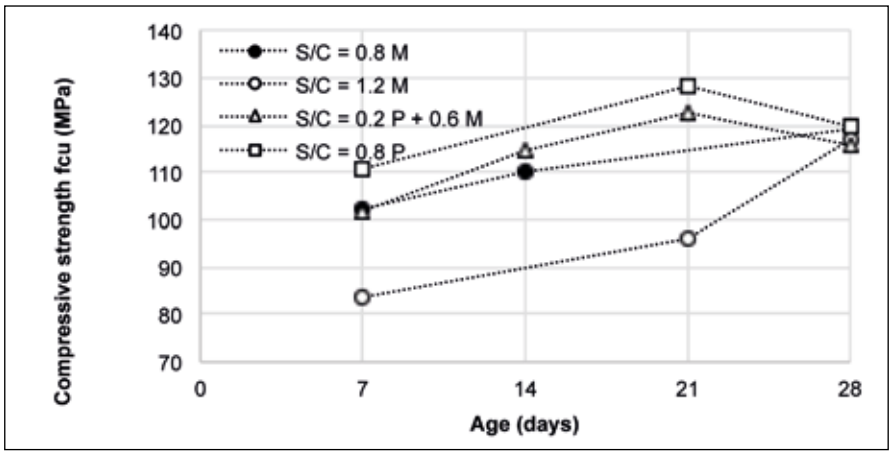

Figure 6: UHPM compressive strength for Phase 1b.

5.1.2. Phase 1b: UHPP base mix performance combined with locally available fine aggregate

The compatibility of the base mix (w/c = 0.22, SF/C = 0.18) with local fine sands is checked in this step by slump flow and compressive strength tests. The sand content was varied in the range 0.8 ≤ S/C = 0.8 and 1.2, and for the case S/C = 0.8, only Phillipi sand (P), only Malmesbury sand (M) and a 1:3 blend were tested. The compressive strength evolution results are shown in Figure 6.

Figure 6 shows a significant reduction in maximum compressive strength from the UHPP base mix strength of more than 140 MPa in Figure 5. It also appears that the fine Phillipi sand leads to an increased maximum strength (5%) above the blended sand. However, the strengths are considered to be insufficient, to an extent indicated by strongly reduced slump flow values from 320 mm for the UHPP base mix, to the range 190 – 228 mm as shown in Table 4.

This indicates that further optimisation is required, to maximize UHPP strength and slump flow, to compensate for less than ideal local sand, as described in section 2.4. For this purpose, the best performing SP is selected next (Phase 1c) according to highest UHPP slump flow, and that SP dosage is optimised in Stage 1e. The interim Phase 1d introduces further strength enhancement by replacing CEM I 42.5N cement with newly available local CEM I 52.5N, and finally reducing the w/c of the base mix from 0.22 to 0.20.

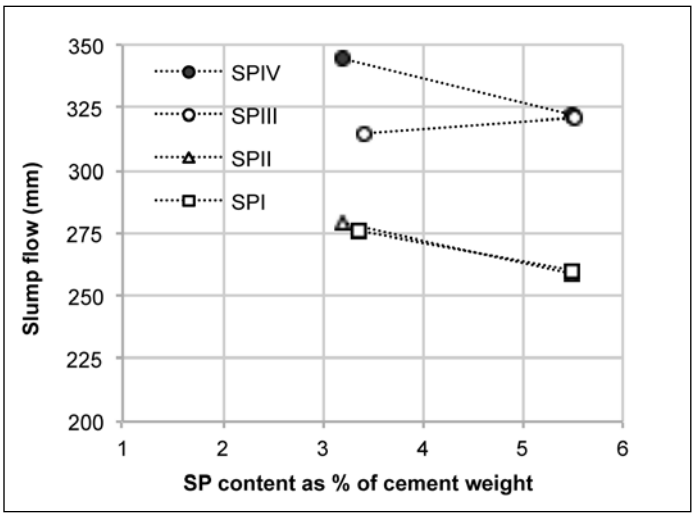

(a)

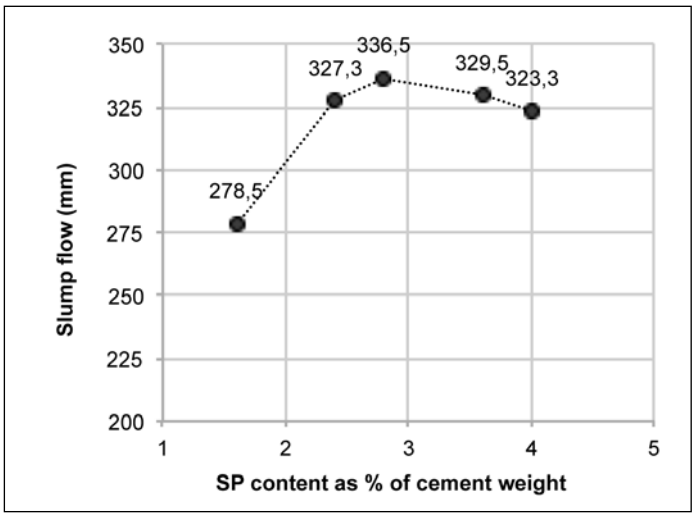

(b)

Figure 7: UHPP slump flow (a) for different SP types and (b) optimisation with SPIV.

5.1.3. Phase 1c – 1e: UHPP improved spread by optimizing SF/C and SP type and dosage

From Phase 1a an indication of higher strength for a higher spread value is seen, for instance for the case of w/c = 0.28 containing a higher SP content, leading to a higher spread value and higher compressive strength. In Phase 1c, the most suited SP type from four available local types is examined in this research, based on slump flow tests for the selected base mix from Phase 1a. See Table 4 for the mix detail for Phase 1c. The results are shown in Figure 7a, where it is apparent that SPIV achieves the highest slump flow for this particular base mix. This SP is selected for further mix optimization in subsequent steps. Cross checks with other SP types are performed from time to time to confirm that SPIV is the most suitable for the UHPC developed here – see Table 4.

As the requirement of higher strength was apparent after Stages 1a and 1b, the newly available CEM I 52.5N was used from here onward as replacement of the CEM I 42.5N cement. In Phases 1d and 1e the option was taken to minimize the w/c ratio and maximize the spread, at the cost of SF, by reducing the SF/C further to 0.16. This was due to the lessons from Stage 1b, which showed significant reduction in slump flow once fine aggregate is added. This is believed not to be a unique option for UHPM and UHPC, which will be investigated further in future, due to the potential strength gain by higher SF/C values seen in Phase 1a, albeit at the cost of reduced slump flow. An acceptable slump flow value of 329 mm is finally found for the Phase 1d optimized UHPP mix, containing CEM I 52.5N at w/c = 0.2, SF/C = 0.16 and SPIV at 3.2% of the cement weight – see Table 4.

From Figure 7a it is not clear what the optimum dosage of SP is, justifying a systematic study. The results are shown in Figure 7b, which confirms an optimum dosage of this type of SP for the UHPP base mix of about 2.8%.

5.2. Phase 2 - Optimization of the UHPM

A slight benefit could be seen in Phase 1b of this research in using the finer Phillipi sand rather than Malmesbury sand. Nevertheless, only Malmesbury sand was used in Phase 2. Optimisation of UHPC containing these local sands is a current, ongoing research focus. An objective of this paper is to illustrate exploitation of non-perfect local ingredient materials for UHPC, which is served well with this choice. This fact becomes clear in Phase 3, when fibre is added to the composite and UHPC which exceeds the strength requirements, is achieved, without heat curing.

From Phase 1b no clear indication of the optimum fine aggregate content could be found. Clearly the maximum amount of sand will be beneficial from a cost point of view. For this reason three contents were tested, ranging from a relatively low value of S/C = 0.6, through a typical value of S/C = 1 to a high value of S/C = 1.4 – see the UHPM descriptions in Table 4. In Figure 8a the slump flow results for these UHPM mixes are shown, decreasing from 336 mm for the optimized UHPP to 294 mm, 247 mm and 203 mm once Malmesbury sand is added in the mentioned respective increasing S/C ratios. Also shown in the graph are results of final slump flow checks that another SP is not as effective as the selected SPIV for the specific mix and dosage. The spread value of UHPM with S/C = 1.4 developed by Wille, *et al*. (2012) is approximately 300 mm, stressing the importance of optimized fine aggregate and UHPP to achieve this.

The compressive strength results are shown in Table 4, and graphically in Figure 8b. From the graph it is apparent that sand content S/C = 0.6 leads to a reduction in compressive strength from 153 MPa of the optimized UHPP base mix also shown in the graph, to 144 MPa of UHPM. Beyond this sand content, its inclusion in UHPM leads to erratic strength evolution, possibly also due to poor dispersion and sensitivity to test cube geometrical imperfection.

5.3. Phase 3 - UHPC

In the final stage, short steel fibres at 1.5% by total volume is added to the optimised UHPM. The resulting compressive strength development up to 28 days in Figure 9a. As comparison, the strength evolution of the finally optimised UHPP and UHPM are shown in the figure as well. The steadily increasing strength development in time is evident of a sound skeleton and bridging of micro-cracks induced by shrinkage of the UHPP. An ultimate strength of 168.7 MPa is achieved at the age of 28 days, succeeding in developing UHPC without heat curing.

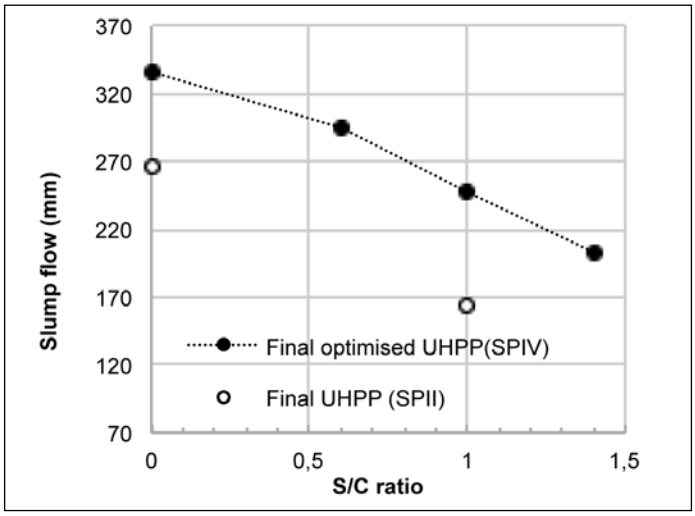

(a) Phase 2 – UHPM Slump flow

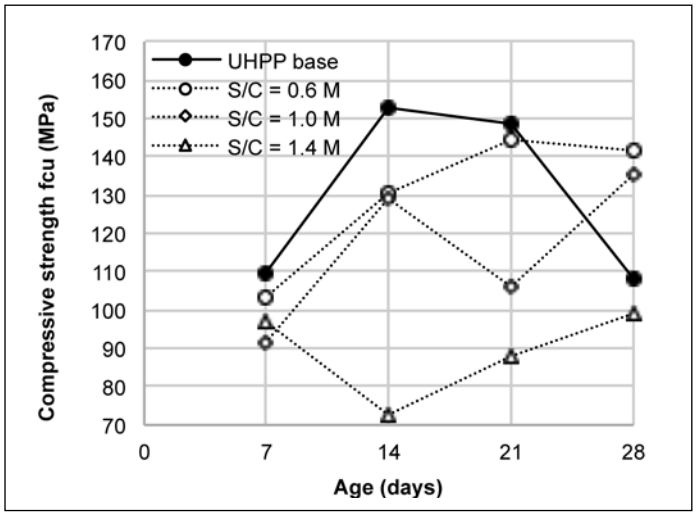

(b) Phase 2 – UHPM strength

Figure 8: UHPM (a) slump flow and (b) compressive strength development.

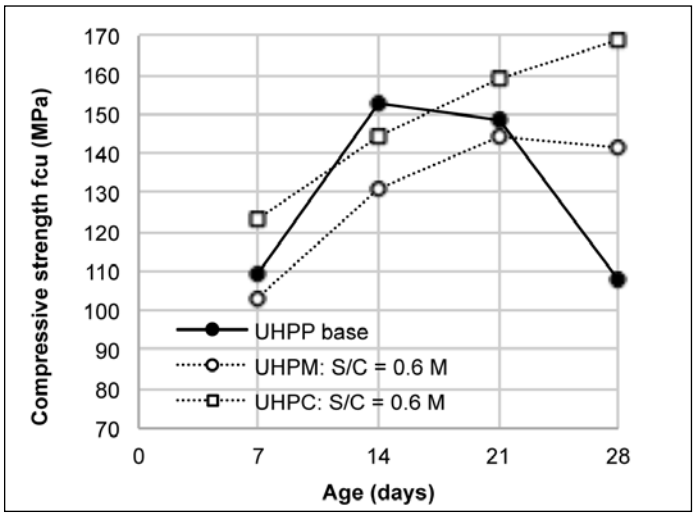

(a) Phase 3 – UHPC, only fine aggregate

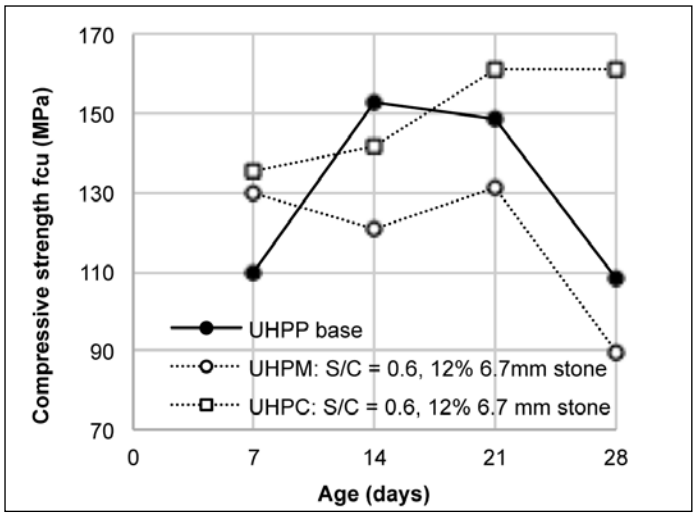

(b) Phase 3 – UHPC, fine & coarse aggregate

Figure 9: Compressive strength development of UHPM containing (a) fine sand only, and (b) fine and coarse aggregate.

Figure 9b shows the results when, in addition to fine aggregate (Malmesbury sand at S/C = 0.6), 12% by volume of small particle stone (6.7 mm) is added to both the mortar (UHPM) and composite (UHPC). Clearly, the UHPM strength evolution is erratic, but that of the UHPC demonstrates that the shortcomings are overcome once the 1.5% steel fibres are added. An ultimate strength of 161 MPa is achieved in this case. This successful achievement of UHPC may be ascribed to the optimised UHPP. Also, the large aggregate particle size of 6.7 mm approaches the requirement that the fibre length is at least 2 to 3 times the aggregate particle size.

The final strength of UHPC is 19% higher than the UHPM strength, by the addition of only 1.5% by volume of short steel fibre. This is a significantly higher increase than reported by Wille *et al*. (2012) of 6.7% increase achieved with 1.5% steel fibres and 9.8% with 2.5% steel fibres, and indicates the effective use of fibres in this research.

6. CONCLUSION

The research reported here produced UHPC without heat treatment, using locally available binder materials, fine aggregate and super-plasticisers, together with imported short steel fibres. Due to chemical and geometrical properties not falling within optimal ranges according to reported guidelines, an alternative strategy is followed here. Instead of avoiding relatively larger UHPC shrinkage, the shrinkage is used to improve the bond stress between steel fibre and the matrix. The following conclusions are drawn:

- It is possible to design UHPC with relatively low C_3S content (61.6% of cement weight), and relatively high C_2S content (17.2%) cement.
- Local available silica fume with specific surface area of 23 ± 3 m^2/g was used successfully in UHPC reported here, while literature reports indicate a preferred value of near half this value (12 m^2/g).
- Probing tests in this research showed that higher paste strength could be achieved with silica fume to cement ratios in the range 0.2-0.25. However, due to the high water demand of the fine local silica fume, a low ratio of 0.16 was successfully used to produce UHPC.
- Fine aggregate from a natural local source and maximum particle size more than 2.4 mm can be successfully used in UHPC, by optimising the UHPP to have the most compatible superplasticiser, cement and silica fume mix. A lower sand content (S/C = 0.6) was used, due to the slump flow reduction to significantly below the preferred threshold of 300 mm.
- The maximum compressive strength of the UHPC achieved in this work (168 MPa) is 19% higher than that of the UHPM, which is a significantly higher contribution by the fibres than values reported in the literature. It is ascribed to the well dispersed, overlapping fibre and the tight skeleton formed of fibre and fine aggregate, whereby fibre bond is enhanced. Paste shrinkage further enhances bond.
- High early age compressive strength at the age of 7 – 14 days, of the water-cured paste is a good indicator of UHPC potential. By introducing a mechanism of shrinkage induced clamping pressure, a bridging effect of steel fibre with adequate lap length and uniform dispersion is achieved. In this way, high compressive strength development is achieved.

Acknowledgement

The research is sponsored by the South African Department of Trade and Industry under the THRIP project ACM, and industry partners AECOM, Element Consulting, PPC and Tubular Track. ▲

REFERENCES

ARTELT, C. and GARCIA, E., 2008. Impact of superplasticizer concentration and of ultra-fine particles on the rheological behaviour of dense mortar suspensions. ***Cement and Concrete Research***, 38(5), pp. 633-642.

BONEN, D. and SARKAR, S.L., 1995. The superplasticizer adsorption capacity of cement pastes, pore solution composition, and parameters affecting flow loss. ***Cement and Concrete Research***, 25(7), pp. 1423-1434.

DE LARRARD, F., 1988. ***Mix-design and properties of very-high performance concrete***, Doctoral Thesis of Ecole Nationale des Ponts et Chaussees.

DE LARRARD, F. and SEDRAN, T., 1994. Optimization of ultra-high-performance concrete by the use of a packing model. ***Cement and Concrete Research***, 24(6), pp. 997-1009.

DE LARRARD, F. and TONDAT, P., 1993. Sur la contribution de la topologie du squelette granulaire à la résistance en compression du béton [On the contribution of the topology of the aggregate skeleton to the compressive strength of concrete]. ***Materials and Structures/Materiaux et Constructions***, 26(9), pp. 505-516.

DUDZIAK, L. and MECHTCHERINE, V., 2008. Mitigation of volume changes of ultra-high performance concrete (UHPC) by using super absorbent polymers. ***Second International Symposium on Ultra High Performance Concrete, Kassel, Germany***, March 05-07 2008, pp. 425-432.

ESPING, O., 2007. ***Early-age properties of self-compacting concrete - Effects of fine aggregate and limestone filler***, Chalmers University of Technology.

GŁODKOWSKA, W. and KOBAKA, J., 2013. Modelling of properties and distribution of steel fibres within a fine aggregate concrete. ***Construction and Building Materials***, 44, pp. 645-653.

GRAYBEAL, B., 2006. ***Material Property Characterization of Ultra-High Performance Concrete***.

GRÜNEWALD, S., 2004. ***Performance-based design of self-compacting fiber reinforced concrete***. PhD thesis, Faculty of Civil Engineering, Delft University of Technology, The Netherlands.

HABEL, K., CHARRON, J., BRAIKE, S., HOOTON, R.D., GAUVREAU, P. and MASSICOTTE, B., 2008. Ultra-high performance fibre reinforced concrete mix design in central Canada. ***Canadian Journal of Civil Engineering***, 35(2), pp. 217-224.

HABEL, K., VIVIANI, M., DENARIÉ, E. and BRÜHWILER, E., 2006. Development of the mechanical properties of an Ultra-High Performance Fiber Reinforced Concrete (UHPFRC). ***Cement and Concrete Research***, 36(7), pp. 1362-1370.

HOLT, E., 2001. ***Early-age autogenous shrinkage of concrete***, University of Washington.

MARKOVIC, I., 2006. ***High-Performance Hybrid-Fibre Concrete - Development and Utilisation***. PhD thesis, Faculty of Civil Engineering, Delft University of Technology, The Netherlands.

MCKEE, D.C., 1969. ***The properties of expansive cement mortar reinforced with random wire fibers***. PhD Thesis edn. U.S.A.: University of Illinois, Urbana.

MINDESS, S. and YOUNG, J.F., eds, 1981. ***Concrete***. First Edition edn. U.S.A.: Prentice Hall.

MORIN, V., COHEN TENOUDJI, F., FEYLESSOUFI, A. and RICHARD, P., 2001. Superplasticizer effects on setting and structuration mechanisms of ultra-high-performance concrete. ***Cement and Concrete Research***, 31(1), pp. 63-71.

PLANK, J., SCHROEFL, C., GRUBER, M., LESTI, M. and SIEBER, R., 2009. Effectiveness of polycarboxylate superplasticizers in ultra-high strength concrete: The importance of PCE compatibility with silica fume. ***Journal of Advanced Concrete Technology***, 7(1), pp. 5-12.

ROMUALDI, J.P. and MANDEL, J.A., 1964. Tensile strength of concrete affected by uniformly distributed closely spaced short lengths of wire reinforcement. ***Journal of the American Concrete Institute***, 61(4), pp. 657-671.

SAKAI, E., AKINORI, N., DAIMON, M., AIZAWA, K. and KATO, H., 2008. Influence of Superplasticizer on the Fluidity of Cements with Different Amount of Aluminate Phase. ***Second International Symposium on Ultra High Performance Concrete***, pp. 85-92.

SCHACHINGER, I., SCHMIDT, K., HEINZ, D. and SCHIESSL, P., 2002. Early age cracking risk and relaxation by restrained autogenous deformations of ultra-high performance concrete, ***6th International Symposium on High Strength / High Performance Concrete*** 2002, pp. 1341-1354.

SCHROEFL, C., GRUBER, M. and PLANK, J., 2008. Structure Performance Relationship of Polycarboxylate Superplasticizers based on Methacrylic Acid Esters in Ultra High Performance Concrete, ***Second International Symposium on Ultra High Performance Concrete*** 2008, pp. 383.

SOLIMAN, A.M. and NEHDI, M.L., 2014. Effects of shrinkage reducing admixture and wollastonite microfiber on early-age behavior of ultra-high performance concrete. ***Cement and Concrete Composites***, 46, pp. 81-89.

STANG, H. 1996. Significance of Shrinkage-Induced Clamping Pressure in Fiber-Matrix Bonding in Cementitious Composite Materials. ***Advanced Cement Based Materials***, 4 (3–4).

TUE, N.V., MA, J. and ORGASS, M, 2008. Influence of Addition Method of Superplasticizer on the Properties of Fresh UHPC, ***Second International Symposium on Ultra High Performance Concrete*** 2008, pp. 93-100.

WILLE, K., NAAMAN, A.E., EL-TAWIL, S. and PARRA-MONTESINOS, G.J., 2012. Ultra-high performance concrete and fiber reinforced concrete: achieving strength and ductility without heat curing. ***Materials and Structures***, 45(3), pp. 309-324.

WILLE, K., NAAMAN, A.E. and PARRA-MONTESINOS, G.J., 2011. Ultra-high performance Concrete with compressive strength exceeding 150 MPa (22 ksi): A simpler way. ***ACI Materials Journal***, 108(1), pp. 46-54.

ZINGG, A., WINNEFELD, F., HOLZER, L., PAKUSCH, J., BECKER, S., FIGI, R. and GAUCKLER, L., 2009. Interaction of polycarboxylate-based superplasticizers with cements containing different C3A amounts. ***Cement and Concrete Composites***, 31(3), pp. 153-162.